Predicting Overall Survival After Conventional Chemoembolization of Intrahepatic Cholangiocarcinoma: The Role of 3D Quantitative Tumor Analysis

Irvin Rexha
Yale University
Fabian Laage-Gaupp
Yale University
Julius Chapiro
Yale University
Milena Anna Miszczuk
Yale University
Johanna Maria Mintje Breugel
Yale University
MingDe Lin
Yale University
Rafael Duran
Johns Hopkins University
Bernhard Gebauer
Charité
Christos Georgiades
Johns Hopkins University
Kelvin Hong
Johns Hopkins University
Nariman Nezami (dr.nezami@gmail.com)
Emory University

Research Article

Keywords: Intrahepatic cholangiocarcinoma (ICC), total tumor volume (TTV), enhancing tumor volume (ETV)

Posted Date: February 23rd, 2021

DOI: https://doi.org/10.21203/rs.3.rs-217136/v1

Version of Record: A version of this preprint was published at Scientific Reports on April 29th, 2021. See the published version at https://doi.org/10.1038/s41598-021-88426-x.

Abstract

This study was designed to assess 3D vs. 1D and 2D quantitative tumor analysis for prediction of overall survival (OS) in patients with ICC who underwent conventional transarterial chemoembolization (cTACE). 73 ICC patients who underwent cTACE were included in this retrospective analysis between Oct 2001 and Feb 2015. The overall and enhancing tumor diameters as well as the maximum cross-sectional and enhancing tumor areas were measured on baseline images. 3D quantitative tumor analysis was used to assess total tumor volume (TTV), enhancing tumor volume (ETV), and enhancing tumor burden (ETB) (ratio between ETV and liver volume). Patients were divided into low (LTB) and high tumor burden (HTB) groups. There was a significant separation between survival curves of the LTB and HTB groups using enhancing tumor diameter (p=0.003), enhancing tumor area (p=0.03), TTV (p=0.03), and ETV (p=0.01). Multivariate analysis showed a hazard ratio of 0.46 (95% CI 0.27–0.78, p=0.004) for enhancing tumor diameter, 0.56 (95% CI 0.33–0.96, p=0.04) for enhancing tumor area, 0.58 (95% CI 0.34–0.98, p=0.04) for TTV, and 0.52 (95% CI 0.30–0.91, p=0.02) for ETV. TTV and ETV as well as largest enhancing tumor diameter and maximum enhancing tumor area reliably predict the OS of patients with ICC after cTACE and could identify ICC patients who are most likely to benefit from cTACE.

Introduction

Intrahepatic cholangiocarcinoma (ICC) is a neoplasm of the epithelial cells of the biliary tract [1-5]. It accounts for 10-20% of all cholangiocarcinoma and is the second most common primary liver cancer [1,4-7]. Patients with ICC are commonly diagnosed at advanced stages of the disease due to unspecific symptoms [4,5,7,8]. Therefore, the survival rates are dismal with an estimated median overall survival (MOS) of 3 to 8 months and fewer than 10% of patients surviving 5 years after diagnosis [8,9]. Surgery still remains the only curative treatment option, however, only 25-35% of ICC patients are eligible for surgical resection at the time of diagnosis [4,5,9]. Systemic chemotherapy using gemcitabine and cisplatin has limited efficacy, with a MOS of 11-12 months [4,8,10,11]. Within the last two decades, lipiodol-based conventional transarterial chemoembolization (cTACE) has emerged as a palliative treatment option. It is increasingly used in combination or as second line treatment after systemic chemotherapy [5,6,8,9,12]. One of the landmark studies in ICC patients demonstrated favorable outcomes for cTACE with a MOS of 12.2 months with MOS of 22 month in responders, when compared to a MOS of 3.3 months for the best supportive care therapy [13].

Given the availability of different treatment options for unresectable ICC, it is crucial to precisely assess the tumor burden and evaluate the treatment outcomes for a more personalized treatment plan and potentially improved outcomes [5,14-16]. Although 1-dimensional (1D) and 2-dimensional (2D) tumor assessment methods have been implemented in the clinical practice for the past decades, these methods have been continuously modified due to subjectivity, lack of reproducibility, and incomplete representation of the tumor [17,18]. Therefore, 3-dimentional (3D) quantitative tumor analysis methods were introduced as a potential solution to address the imprecision in tumor burden assessment [18-20]. The

rationale of 3D quantitative tumor analysis on post-contrast MRI is based on the assumption that viable tumor can be delineated as the enhancing component and used as a quantitative surrogate for the extent of active disease and ultimately as an indicator for tumor response post cTACE. Accordingly, the outcome of cTACE can be visualized and assessed as a decrease in tumor enhancement on MRI, as successful cTACE and locoregional chemotherapy delivery are expected to induce tumor necrosis [21-24].

Predicting therapeutic outcomes before cTACE and its potential efficacy is important and would allow for a more accurate and individualized patient allocation to this therapy. Thus, this study aimed to evaluate the performance of 3D vs. 1D and 2D methods for quantitative tumor analysis of contrast-enhanced MRI for the prediction of overall survival (OS) in patients with ICC who underwent cTACE.

Methods And Materials

Study design

This single-institutional study was conducted retrospectively and received institutional review board (IRB) approval from the Yale School of Medicine. Data collection and analysis were conducted in compliance with the Health Insurance Portability and Accountability Act (HIPPA). Study design was in agreement with the Standards for Reporting of Diagnostic Accuracy guidelines [31]. Written informed consent from all subjects was waived by the IRB committee of Yale School of Medicine due to the retrospective nature of this study.

Study cohort

Initially, a total of 122 consecutive patients with biopsy-proven ICC lesions and history of systemic chemotherapy who underwent cTACE between October 2001 and February 2015 were evaluated. The following inclusion criteria were then applied: unresectable ICC (i.e. patients with mixed ICC and hepatocellular carcinoma were not included), naïve to locoregional treatment including percutaneous ablations or other intra-arterial therapies than cTACE as well as stereotactic body radiation therapy, and preprocedural multi-phase contrast-enhanced MRI with adequate/artifact-free image quality adequate for 3D quantitative tumor analysis.

Clinical and laboratory evaluation and staging

All patients had a complete clinical examination and baseline laboratory workup including bilirubin, albumin, and International Normalized Ratio (INR). Initial diagnosis of ICC was made on imaging and confirmed on pathology. Furthermore, the Child-Pugh classification for liver function and The Eastern Cooperative Oncology Group (ECOG) performance status were documented for each patient. The stage of disease was assessed using the Union for International Cancer Control (UICC) staging system.

cTACE protocol

All patients were discussed in the multidisciplinary tumor-board, and enrolled to undergo cTACE based on final consensus. The interventions were performed by the same interventional radiologist (with more than 20 years of experience) in a dedicated interventional radiology suite (Philips IR suites). After local anesthesia with lidocaine 1%, access was obtained through the common femoral artery via a 5 Fr vascular sheath, followed by a 0.035-in. guide wire in Seldinger technique. For orientation purposes, diagnostic angiography of the superior mesenteric artery and celiac trunk was obtained using a 5 Fr catheter to selectively advance into the tumor-supplying hepatic artery. Selective catheterization was achieved by placing a microcatheter and obtaining further imaging in order to more precisely target and spare healthy liver parenchyma. All patients were treated with a cTACE-protocol comprising of a 1:1 mixture of 50 mg doxorubicin (Adriamycin®, Pharmacia & Upjohn) and 10 mg of mitomycin-C with 10mL of iodized oil (Lipiodol®, Guerbet). This was followed by administration of 100–300 μm diameter microspheres (Embosphere®, Merit Medical); until complete stasis was reached, as the technical end point.

Imaging protocol

A standardized liver MRI protocol was performed in all patients enrolled using a 1.5T scanner (Magnetom Avanto, Siemens) with a phased array torso coil (repetition time ms/echo time ms, 5.77/2.77; field of view 320-400 mm; matrix 192 x 160; slice thickness 2.5 mm; receiver bandwidth 64 kHz; flip angle 10^{o}). The protocol included single-shot breath-held gradient-echo diffusion weighted echo-planar images, axial T2-weighted fast spin-echo images, and unenhanced and contrast-enhanced (0.1 mmol/kg intravenous gadopentetate; Magnevist; Bayer) breath-held axial T1-weighted 3D fat-suppressed spoiled gradient-echo images in the hepatic arterial, portal venous and delayed phases (20s, 70s, and 180s, respectively)[24,32,33].

Image analysis

All measurements were conducted using standard electronic calipers on Digital Imaging in Communications and Medicine (DICOM) files. Different sequences were assessed to distinguish between tumor enhancement and other hyperintense T1 signal abnormality (such as hemorrhage) in order to evaluate the true extent of tumor burden. If multiple lesions were present, the three largest lesions were assessed and the sum of total lesions in each patient was then processed in the analysis. For tumor burden analysis using each technique (1D, 2D and 3D), the most dominantly enhancing axial MRI sequence was used in each patient, since the enhancement pattern of ICC depends on tumor size and can vary accordingly [34]. The largest overall tumor diameter (1D) and maximum cross-sectional area (2D), as well as the largest enhancing tumor diameter (1D) and maximum enhancing tumor area (2D) were measured by two radiological readers (XX with 5 years of experience and YY with 4 years of experience in abdominal MRI, respectively), using the RadiAnt™ DICOM Viewer (Medixant). The numbers used for the final analysis were the consensus of the simultaneous measurement and discussion of both readers; both readers were blinded to all clinical data.

For the 3D tumor assessment, a 3D quantitative semiautomatic tumor analysis software was used (IntelliSpacePortal V8, Philips ICAP) [19]. The total tumor volume (TTV) and enhancing tumor volume (ETV) were assessed by an independent radiological reader with 1 year of experience with the software (ZZ). Three-dimensional segmentation-masks of the tumors were created to determine TTV and ETV using qEASL (Figure 2). Generally, the area within the segmentation-mask is considered the TTV and expressed in cubic centimeters (cm^3). ETV was assessed using qEASL calculation in cubic centimeters (cm^3)[11]. Initially, axial native MRI T1-weighted images were subtracted from axial enhancing phase images to remove false-positive background enhancement. After subtraction, 3D tumor segmentation-masks were used to select a region of interest (ROI) consisting of a 1 cm^3 sized cube placed manually within non-tumor liver parenchyma as described previously in the literature [35]. The ROI within the background liver parenchyma sets a cut-off value based on intensity that is used as a reference to calculate the ETV within the segmentation-masks of the tumors (Figure 2). After setting the ROI, the software automatically generates a color map of enhancing regions within the segmented 3D tumor mask. The non-enhancing and necrotic areas of the tumor were represented in blue, whereas enhancing and thus viable parts of the tumor were represented in red. The quantitative output resulted in volumetric values indicative of tumor enhancement.

To evaluate the enhancing tumor burden (ETB) within the liver, the total liver volume (TLV) was calculated using a software prototype (Medisys, Philips Research), that automatically generates a segmentation-mask of the entire liver. The software allows contraction and expansion of the segmentation-mask around control-points within the liver or its contour. Thereby, the mask can be manually adjusted by the reader to fully include all anatomical parts of the organ. The true volume of the segmented liver will be calculated and enunciated in cubic centimeters (cm^3). The ETB (%) was calculated using the following formula:

$$\text{ETB}\,(\%) = \frac{\text{ETV}\,(\text{cm}^3)}{\text{TLV}\;\;(\text{cm}^3)} \text{x}\;100\%$$

This formula takes into account the ETV in relation to the TLV by calculating their ratio. For comparative purposes, patients were divided into low tumor burden (LTB) and high tumor burden (HTB) groups based on cut-off points defined for each 1D, 2D, ad 3D method.

Statistical analysis

Statistical analysis of the data was performed using SAS (SAS Institute, Version 9.4.3) and IBM SPSS Statistics (IBM, Version 23.0). Qualitative variables were presented as absolute numbers and percentages. Continuous variables were described by using mean ± standard deviation or median (range). Additionally, the Cox proportional hazard model was used to determine the predictive value of TTV, ETV, and ETB. Survival was calculated based on the interval between the date of embolization and death or last known alive date. The OS and cumulative survival analysis were calculated and represented using Kaplan-Meier curves, and the log-rank test was utilized to further contrast these survival curves. Q

statistics was used to estimate the most significant cutoff values for each tumor assessment method, then the best area under the curve calculated by receiver operating characteristic (ROC) curve analysis was confirmed and utilized for every tumor assessment method to determine the optimal cutoff point for patient categorization into LTB and HTB groups, based on improved survival after cTACE. The demographic characteristics, child-Pugh classification, and tumor stage were considered for multivariate analysis. A *p*-value of less than 0.05 was considered statistically significant.

Results

Patient characteristics and clinical outcome

Out of 122 patients, 49 did not meet our inclusion criteria. Eight patients were excluded because 5 had prior partial hepatectomy and 3 had prior Yttrium-90 radioembolization. Forty-one patients had missing images or inadequate/missing MRI sequences; 9 patients were missing baseline imaging, 9 patients were missing critical MRI sequences, and 23 patients had severe motion artifacts. After excluding these 49 patients, a total of 73 patients were enrolled into the final analysis. The study flowchart for inclusion is shown in Figure 1.

The patients' baseline characteristics are summarized in Table 1. Mean patient age was 60.32 ± 12.04 years (range 29 – 83 years) and the MOS was 11 months (range 0.6-52.2 months; 95% CI 7-14 months). Seven patients had cirrhosis. Primary sclerosing cholangitis was the most common risk factor, affecting 19 (26%) of the included patient cohort. The majority of the ICC patients had ECOG scores of 0 or 1 as well as Child-Pugh Class A. All patients received Gemcitabine/Cisplatin-based systemic therapy prior to cTACE (Range 1-11 cycles). Eleven patients additionally received FOLFOX/FOLFIRI-based second line chemotherapy. The median time interval between pre-interventional imaging and cTACE was 14 days.

Table 1. Patients' demographic characteristics		
Parameter	*N*	*(%)*
Demographics		
Number of patients	73	(100)
Age		
< 65	43	(58.9)
≥ 65	30	(41.10)
Gender		
Female	45	(61.64)
Male	28	(38.36)
Ethnicity		
African-American	6	(8.22)
Asian/Pacific-Islander	3	(4.11)
Hispanic	2	(2.74)
Other	8	(10.96)
White	54	(73.97)
Underlying chronic liver disease		
HBV	4	(5.48)
HCV	4	(5.48)
HIV	4	(5.48)
Alcohol	5	(6.85)
NASH	8	(10.96)
Cirrhosis	7	(9.59)
Primary sclerosing cholangitis	26	(35.62)
ECOG score		
0	55	(75.34)
1	13	(17.81)
2	5	(6.85)
Child-Pugh class		

A	62	(84.93)
B	10	(13.70)
C	1	(1.370)
UICC Stage		
0	0	(0)
IA	0	(0)
IB	4	(5.48)
IIA	12	(16.44)
IIB	25	(34.25)
III	0	(0)
IV	32	(43.84)
Average number of cTACE sessions	1.89	(1-5)

Tumor characteristics

Table 2 summarizes the tumor characteristics evaluated in this study.

Table 2. 1D, 2D, and 3D tumor burden assessment

Assessment Technique	*Mean ± SD*	*Range*
1D Tumor Assessment		
Mean Overall Tumor Diameter (cm)	12.33 ± 6.60	2.44-36.04
Mean Enhancing Tumor Diameter (cm)	9.35 ± 4.64	3.56-28.21
2D Tumor Assessment		
Mean Max. Cross-Sectional Area (cm^2)	64.31 ± 54.73	2.87-353.53
Mean Enhancing Tumor Area (cm^2)	31.87 ± 25.77	4.12-110.81
3D Tumor Assessment		
Mean Total Tumor Volume (cm^3)	629.38 ± 748.65	7.78-3566.81
Mean Enhancing Tumor Volume (cm^3)	289.44 ± 432.79	0.17-2176.77
Mean Enhancing Tumor Burden (%)	11.63 ± 13.90	0.02-72.87

A total of 419 lesions were measured and analyzed using 1D, 2D, and 3D tumor assessment methods. The mean number of tumor lesions per patient was 1.91. The patients were enrolled into the LTB and HTB groups according to cut-off values calculated by Q statistic and obtained from ROC curve analysis for 1D, 2D, and 3D assessment methods (Table 3 and Figure 3).

Table 3. Methods of patient assignment to LTB and HTB in each tumor assessment method

Assessment method		*LTB*	*HTB*	*Log-rank p-value*
1D	Overall Tumor Diameter (cm)	≤ 9.3	> 9.3	0.02
	Enhancing Tumor Diameter (cm)	≤ 8.5	> 8.5	0.003
2D	Maximum Cross-Sectional Area (cm^2)	≤ 50	> 50	0.15
	Enhancing Tumor Area (cm^2)	≤ 25	> 25	0.03
3D	Total Tumor Volume (cm^3)	≤ 410	> 410	0.03
	Enhancing Tumor Volume (cm^3)	≤ 275	> 275	0.01
	Enhancing Tumor Burden (%)	≤ 10	> 10	0.11

LTB: low tumor burden, HTB: high tumor burden, 1D: 1-dimensional, 2D: 2-dimensional, 3D: 3-dimensional.

Survival Analysis

1D tumor assessment

When using overall tumor diameter with a cutoff of 9.32 cm, the MOS was 1.54 times longer for the LTB group compared to the HTB group (17.18 months for LTB; 11.17 months for HTB groups, p=0.02). Multivariate analysis showed a HR of 0.51 (95% CI 0.28–0.92; p=0.03) for overall tumor diameter. The mortality ratio of the LTB group was 49% lower than in the HTB group (Figure 4. A).

Based on the largest enhancing tumor diameter with the cutoff of 8.7 cm, the MOS of the LTB group was 1.79 times higher than the MOS of the HTB group (17.18 vs. 9.62 months for LTB and HTB groups, respectively; p=0.003). Comparison of the survival curves between the two groups via the log-rank test revealed significant separation in the survival curves (p=0.003; Figure 4. B). Multivariate analysis showed a HR of 0.46 (95% CI 0.27–0.78; p=0.004) for maximum enhancing tumor diameter. The mortality ratio for ICC patients with LTB was 54% lower than patients with HTB (Figure 4. B).

2D tumor assessment

The MOS of the LTB group was not significantly different from the HTB group based on the maximum cross-sectional tumor area and cutoff of 51.7 cm^2 (14.46 vs. 10.97 months for LTB and HTB groups,

respectively; p=0.15 on log-rank test), with the multivariate analysis demonstrating a HR of 0.67 (95% CI 0.40–1.15, p=0.15). Although the mortality ratio in the LTB group was 33% lower than the HTB group (Figure 4. C), it was not statistically significant.

Based on the maximum enhancing tumor area and the cutoff of 25.4 cm^2, the MOS in the LTB group was 1.79 times higher than the HTB group (17.12 vs. 9.56 months for LTB and HTB, respectively; p=0.03), with a HR of 0.56 (95% CI 0.33–0.96: p=0.04). Thus, the mortality ratio was 44% lower for the LTB group, when compared to the HTB group (Figure 4. D).

3D tumor assessment

The MOS of the LTB group based on the TTV cutoff value of 417 cm^3 was significantly higher than in the HTB group (15.41 vs. 8.15 months, respectively; p=0.03 on log-rank test). This means that the MOS for ICC patients in the LTB group was 1.89 times higher than the HTB group. Multivariate analysis showed a HR of 0.58 (95% CI 0.34–0.98, p=0.04) for TTV. The mortality ratio in the LTB group was 42% lower than the HTB group (Figure 4. F).

Categorizing ICC patients into the LTB and HTB groups based on The ETV cutoff value of 250 cm^3 via 3D quantitative analysis revealed a MOS of 14.46 months for the LTB group and 9.56 months for the HTB group, respectively. The MOS of the LTB group was 1.51 times higher than the HTB group (p=0.01). There was a significant separation between survival curves of the two groups (p=0.01 on log-rank test). Multivariate analysis showed a HR of 0.52 (95% CI 0.30–0.91, p=0.02) for ETV, corresponding to a 48% lower mortality ratio for the LTB group when compared to the HTB group (Figure 4. E).

Categorizing the patients into LTB and HTB based on the ETB cutoff value of 10.4% demonstrated a MOS of 14.42 months for the LTB group and 9.63 months for the HTB group (p=0.11 on log-rank test). The MOS was 1.50 times longer for the LTB group compared to the HTB group, though this was not statistically significant. Multivariate analysis showed a HR of 0.65 (95% CI 0.38–1.10, p=0.11) for ETB. The mortality ratio was 35% lower for the LBT group compared to the HBT group (Figure 4. G).

Discussion

Our findings showed that the 3D quantitative biomarkers TTV and ETV, as well as the largest overall tumor diameter, enhancing tumor diameter, and maximum enhancing tumor area, on the baseline images are strong predictors of OS in ICC patients who underwent cTACE. Thereby, stratifying ICC patients into the LTB and HTB groups based on TTV and ETV could be utilized to predict which ICC patients would most likely benefit from improved survival following cTACE and guide a more personalized treatment plan for ICC patients.

Our findings also indicated that the largest enhancing tumor diameter, maximum enhancing tumor area, and 3D tumor burden assessment methods focused on tumor enhancement for evaluation of response more reliably predict post-therapeutic outcomes and achieve significant separation of survival curves

between patients with LTB and HTB when compared to other tumor assessment methods that do not consider enhancement. There was a significant separation of survival curves when the ICC patients were categorized into the LTB and HTB groups based on the largest enhancing tumor diameter from the modified Response Evaluation Criteria in Solid Tumors (mRECIST, 1D assessment method) and enhancing tumor area calculated based on European Association for the Study of the Liver (EASL, 2D assessment method). This circumstance is generally important to consider in practical implementation of tumor assessment, as 1D and 2D techniques are ubiquitous. In concordance, the separation of survival curves was significant when using the 3D quantitative ETV for categorizing ICC patients into the LTB and HTB groups. The good predictive performance of ETV may be related to the fact that enhancement of the tumor on imaging indirectly reflects tumor perfusion and vascularity which is effectively targeted by cTACE. Furthermore, smaller lesions are more likely to be embolized entirely and allow for more complete delivery of chemotherapeutic agents through a limited number of tumor-feeding arteries, compared to larger and more necrotic lesions which may have multiple tumor-feeding arteries or substantially lower hepatic functional reserve due to larger overall tumor burden. Conceivably, cTACE could result in a more complete necrosis in ICC patients with LTB, which explains the corresponding improved OS in this group. ETV, based on 3D quantitative analysis, is an accurate method of predicting which lesion is most likely to respond to cTACE, as it provides more precise indirect information on the perfusion of the tumor by calculating its enhancement pattern [25]. If confirmed in larger cohorts, 3D quantitative assessment of ICC tumor burden could be used as an early stratification instrument for allocation of ICC patients into LTB and HTB groups, with the former group possibly benefiting the most from cTACE monotherapy while the latter group may benefit from combination therapies or systemic chemotherapy.

Although the predictive values of enhancement based 1D and 2D tumor assessment methods were statistically significant, their inherent imprecision has been reported in prior studies, as these methods lack objectivity and do not reflect the entire tumor volume [17-20]. In order to address these shortcomings, 3D quantitative tumor analysis methods were developed. Three-dimensional quantitative tumor analysis is more reliable and is associated with better inter-reader reproducibility and accuracy in tumors such as hepatocellular carcinoma, metastatic neuroendocrine tumors, metastatic colorectal cancer, metastatic renal cell carcinoma, and now ICC [20,26-29]. Furthermore, the precision of 3D quantitative tumor analysis for assessment of tumor necrosis in hepatic malignancies treated with TACE has been described in earlier reports [24]. The semi-automated nature of 3D quantitative tumor analysis segmentation software allows it to automatically generate tumor-masks that can then be modified by radiological readers, combining computer-assisted efficacy and human radiological experience [24]. Additionally, the automated subtraction of non-contrast phases from contrast-enhanced MRI phases allows for more precise and effective assessment of tumor enhancement by mitigating the impact of non-contrast/background hyperenhancement [30]. As volumetric methods rely on enhancement-based functions, 3D tumor quantification can be translated onto other diagnostic modalities, including multi-detector CT and intra-procedural cone-beam CT [20]. In this study, multi-lesion 3D tumor assessment of the entire tumor burden was conducted for every patient, in order to more precisely predict outcomes. Therefore, implementation

of computer-assisted 3D quantitative assessment could introduce a new level of workflow-efficiency and clinical relevance for tumor enhancement on baseline imaging when assessing ICC tumor burden.

This study has several limitations. Due to its retrospective Due to its , the patient populations were inhomogeneous in their disease history, background characteristics, and MRI protocol; in-depth multivariate analysis was performed to reduce the effect of these heterogeneities and counter these limitations. Additionally, this study only evaluated patients treated with cTACE thus results and conclusion cannot be applied to ICC patients treated with or considered for other forms of IAT, including bland embolization, drug-eluting beads, transarterial chemoembolization, or radioembolization with Yttrium 90.

In conclusion, total tumor volume and enhancing tumor volume show great promise as strong predictors of overall survival in patients with ICC undergoing cTACE. Inclusion of 3D quantitative tumor analysis in guidelines for tumor burden and response assessment in patients with ICC should be considered, given the accuracy and reproducibility of 3D quantitative tumor analysis method.

Declarations

Additional Information (Competing Interest Statements)

N.N., R.D., F.L-G., B.G., C.G., K.H. have no conflicts of interest to declare. **M.L.** was an employee of Phillips Research North America and is currently employed at Visage Imaging, Inc. **M.L.** has received grants from the National Institutes of Health (NIH/NCI R01 CA206180). **I.R.** and **M.A.M** have received grants from the Rolf W. Guenther Stiftung. **J.M.M.vB** had received the Academy Van Leersum grant. **J.C.** has received grants from the National Institutes of Health (NIH/NCI R01 CA206180), the Society of Interventional Oncology, the German-Israeli Foundation for Scientific Research and Development, Guerbet Healthcare, Boston Scientific and Philips Healthcare.

Author Contributions

IR: segmentation and 3D image analysis and drafting the manuscript

FLG: 1D and 2d image analysis, and revision of the manuscript

JC: Concept, supervising the study, and revision of the manuscript

MAM: Helped segmentation and 3D image analysis

JMMB: Helped segmentation and 3D image analysis

ML: Developing 3D image analysis software and supervising 3D image analysis

RD: Helped the 3D image analysis

BG: Supervising the 3D image analysis

CG: supervised the clinical data extraction

KH: supervised the clinical data extraction

NN: Concept, 1D and 2D image analysis, supervise 3D image analysis, revise the manuscript

References

1. Bergquist, A. & von Seth, E. Epidemiology of cholangiocarcinoma. *Best Pract Res Clin Gastroenterol.* **29**, 221–232 https://doi.org/10.1016/j.bpg.2015.02.003 (2015).
2. Zhang, H., Yang, T., Wu, M. & Shen, F. Intrahepatic cholangiocarcinoma: Epidemiology, risk factors, diagnosis and surgical management. *Cancer Lett.* **379**, 198–205 https://doi.org/10.1016/j.canlet.2015.09.008 (2016).
3. Wirth, T. C. & Vogel, A. Surveillance in cholangiocellular carcinoma. *Best Pract Res Clin Gastroenterol.* **30**, 987–999 https://doi.org/10.1016/j.bpg.2016.11.001 (2016).
4. Rizvi, S., Khan, S. A., Hallemeier, C. L., Kelley, R. K. & Gores, G. J. Cholangiocarcinoma - evolving concepts and therapeutic strategies. *Nat Rev Clin Oncol.* **15**, 95–111 https://doi.org/10.1038/nrclinonc.2017.157 (2018).
5. Blechacz, B. & Cholangiocarcinoma Current Knowledge and New Developments. *Gut Liver.* **11**, 13–26 https://doi.org/10.5009/gnl15568 (2017).
6. Rizvi, S. & Gores, G. J. Pathogenesis, diagnosis, and management of cholangiocarcinoma. *Gastroenterology.* **145**, 1215–1229 https://doi.org/10.1053/j.gastro.2013.10.013 (2013).
7. Massarweh, N. N. & El-Serag, H. B. Epidemiology of Hepatocellular Carcinoma and Intrahepatic Cholangiocarcinoma. *Cancer Control.* **24**, 1073274817729245 https://doi.org/10.1177/1073274817729245 (2017).
8. Doherty, B., Nambudiri, V. E. & Palmer, W. C. Update on the Diagnosis and Treatment of Cholangiocarcinoma. *Curr Gastroenterol Rep.* **19**, 2 https://doi.org/10.1007/s11894-017-0542-4 (2017).
9. Ierardi, A. M. *et al.* The role of interventional radiology in the treatment of intrahepatic cholangiocarcinoma. *Med Oncol.* **34**, 11 https://doi.org/10.1007/s12032-016-0866-1 (2017).
10. Razumilava, N., Gores, G. J. & Cholangiocarcinoma *Lancet.* **383**, 2168–2179 https://doi.org/10.1016/S0140-6736(13)61903-0 (2014).
11. Valle, J. *et al.* Cisplatin plus gemcitabine versus gemcitabine for biliary tract cancer. *N Engl J Med.* **362**, 1273–1281 https://doi.org/10.1056/NEJMoa0908721 (2010).
12. Vogl, T. J. *et al.* Transarterial chemoembolization in the treatment of patients with unresectable cholangiocarcinoma: Results and prognostic factors governing treatment success. *Int J Cancer.* **131**, 733–740 https://doi.org/10.1002/ijc.26407 (2012).

13. Park, S. Y. *et al.* Transarterial chemoembolization versus supportive therapy in the palliative treatment of unresectable intrahepatic cholangiocarcinoma. *Clin Radiol.* **66**, 322–328 (2011).
14. Ma, J. *et al.* Intraarterial Liver-Directed Therapies: The Role of Interventional Oncology. *Ochsner J.* **17**, 412–416 (2017).
15. Nezami, N. *et al.* Y-90 radioembolization dosimetry using a simple semi-quantitative method in intrahepatic cholangiocarcinoma: Glass versus resin microspheres. *Nuclear Medicine and Biology.* **59**, 22–28 https://doi.org/10.1016/j.nucmedbio.2018.01.001 (2018).
16. Nezami, N., Camacho, J. C., Kokabi, N., El-Rayes, B. F. & Kim, H. S. Phase Ib trial of gemcitabine with yttrium-90 in patients with hepatic metastasis of pancreatobiliary origin. *Journal of Gastrointestinal Oncology.* **10**, 944–956 https://doi.org/10.21037/jgo.2019.05.10 (2019).
17. Hickey, R. *et al.* Cancer concepts and principles: primer for the interventional oncologist-part I. *J Vasc Interv Radiol.* **24**, 1157–1164 https://doi.org/10.1016/j.jvir.2013.04.024 (2013).
18. Stroehl, Y. W., Letzen, B. S., van Breugel, J. M., Geschwind, J. F. & Chapiro, J. Intra-arterial therapies for liver cancer: assessing tumor response. *Expert Rev Anticancer Ther.* **17**, 119–127 https://doi.org/10.1080/14737140.2017.1273775 (2017).
19. Lin, M. *et al.* Quantitative and volumetric European Association for the Study of the Liver and Response Evaluation Criteria in Solid Tumors measurements: feasibility of a semiautomated software method to assess tumor response after transcatheter arterial chemoembolization. *J Vasc Interv Radiol.* **23**, 1629–1637 https://doi.org/10.1016/j.jvir.2012.08.028 (2012).
20. Tacher, V. *et al.* Semiautomatic volumetric tumor segmentation for hepatocellular carcinoma: comparison between C-arm cone beam computed tomography and MRI. *Acad Radiol.* **20**, 446–452 https://doi.org/10.1016/j.acra.2012.11.009 (2013).
21. Savic, L. J., Chapiro, J. & Geschwind, J. H. Intra-arterial embolotherapy for intrahepatic cholangiocarcinoma: update and future prospects. *Hepatobiliary Surg Nutr.* **6**, 7–21 https://doi.org/10.21037/hbsn.2016.11.02 (2017).
22. Miyayama, S. Ultraselective conventional transarterial chemoembolization: When and how? *Clin Mol Hepatol.* https://doi.org/10.3350/cmh.2019.0016 (2019).
23. Vogl, T. J. & Gruber-Rouh, T. H. C. C. Transarterial Therapies-What the Interventional Radiologist Can Offer. *Dig Dis Sci.* **64**, 959–967 https://doi.org/10.1007/s10620-019-05542-5 (2019).
24. Chapiro, J. *et al.* Radiologic-pathologic analysis of contrast-enhanced and diffusion-weighted MR imaging in patients with HCC after TACE: diagnostic accuracy of 3D quantitative image analysis. *Radiology.* **273**, 746–758 https://doi.org/10.1148/radiol.14140033 (2014).
25. Tacher, V. *et al.* Comparison of Existing Response Criteria in Patients with Hepatocellular Carcinoma Treated with Transarterial Chemoembolization Using a 3D Quantitative Approach. *Radiology.* **278**, 275–284 https://doi.org/10.1148/radiol.2015142951 (2016).
26. Fleckenstein, F. N. *et al.* 3D Quantitative tumour burden analysis in patients with hepatocellular carcinoma before TACE: comparing single-lesion vs. multi-lesion imaging biomarkers as predictors of patient survival. *Eur Radiol.* **26**, 3243–3252 https://doi.org/10.1007/s00330-015-4168-3 (2016).

27. Sahu, S. *et al.* Imaging Biomarkers of Tumor Response in Neuroendocrine Liver Metastases Treated with Transarterial Chemoembolization: Can Enhancing Tumor Burden of the Whole Liver Help Predict Patient Survival? *Radiology.* **283**, 883–894 https://doi.org/10.1148/radiol.2016160838 (2017).
28. Chapiro, J. *et al.* Early survival prediction after intra-arterial therapies: a 3D quantitative MRI assessment of tumour response after TACE or radioembolization of colorectal cancer metastases to the liver. *Eur Radiol.* **25**, 1993–2003 https://doi.org/10.1007/s00330-015-3595-5 (2015).
29. Fleckenstein, F. N. *et al.* Renal Cell Carcinoma Metastatic to the Liver: Early Response Assessment after Intraarterial Therapy Using 3D Quantitative Tumor Enhancement Analysis. *Transl Oncol.* **9**, 377–383 https://doi.org/10.1016/j.tranon.2016.07.005 (2016).
30. Duran, R. *et al.* Uveal Melanoma Metastatic to the Liver: The Role of Quantitative Volumetric Contrast-Enhanced MR Imaging in the Assessment of Early Tumor Response after Transarterial Chemoembolization. *Transl Oncol.* **7**, 447–455 https://doi.org/10.1016/j.tranon.2014.05.004 (2014).
31. Cohen, J. F. *et al.* STARD 2015 guidelines for reporting diagnostic accuracy studies: explanation and elaboration. *BMJ Open.* **6**, e012799 https://doi.org/10.1136/bmjopen-2016-012799 (2016).
32. Pandey, A. *et al.* Baseline Volumetric Multiparametric MRI: Can It Be Used to Predict Survival in Patients with Unresectable Intrahepatic Cholangiocarcinoma Undergoing Transcatheter Arterial Chemoembolization? *Radiology.* **289**, 843–853 https://doi.org/10.1148/radiol.2018180450 (2018).
33. Pandey, A. *et al.* Unresectable Intrahepatic Cholangiocarcinoma: Multiparametric MR Imaging to Predict Patient Survival. *Radiology.* **288**, 109–117 https://doi.org/10.1148/radiol.2018171593 (2018).
34. Ni, T. *et al.* Different MR features for differentiation of intrahepatic mass-forming cholangiocarcinoma from hepatocellular carcinoma according to tumor size. *Br J Radiol.* **91**, 20180017 https://doi.org/10.1259/bjr.20180017 (2018).
35. Chockalingam, A. *et al.* Radiologic-pathologic analysis of quantitative 3D tumour enhancement on contrast-enhanced MR imaging: a study of ROI placement. *Eur Radiol.* **26**, 103–113 https://doi.org/10.1007/s00330-015-3812-2 (2016).

Figures

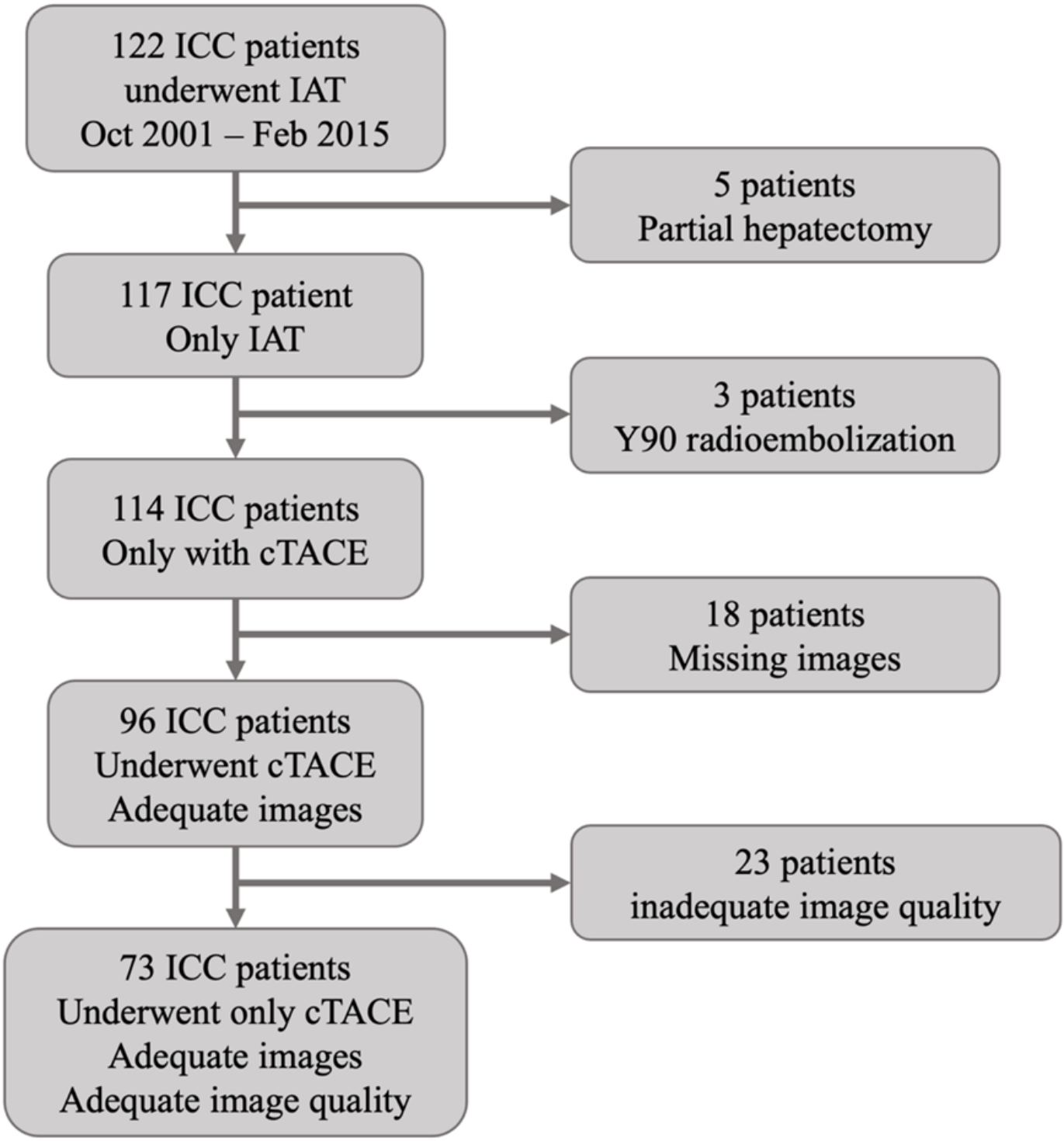

Figure 1

Study flowchart showing number of patients excluded based on exclusion criteria; 73 ICC patients included in final analysis.

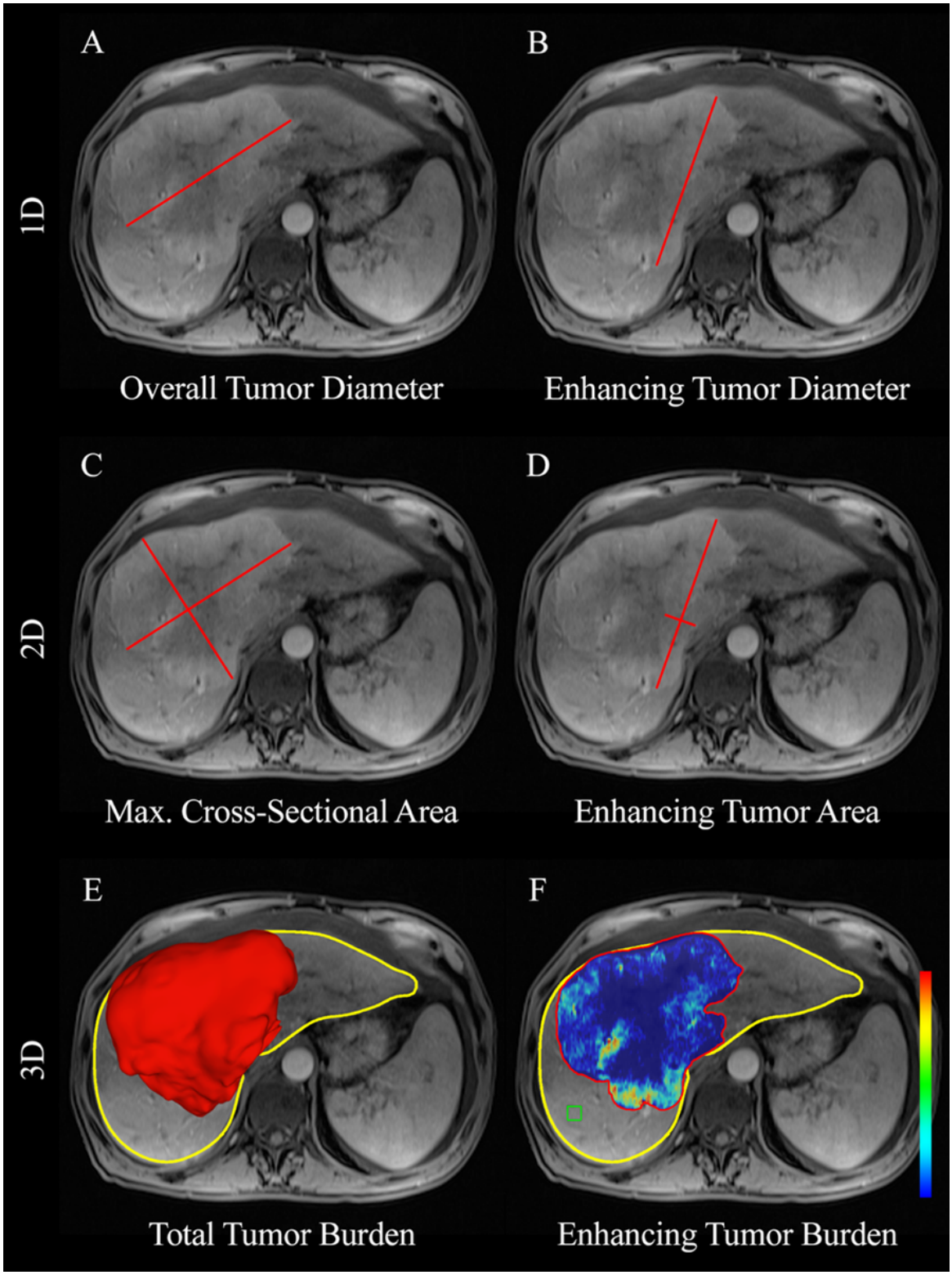

Figure 2

Methods of tumor assessment on enhancement-based MRI. Figures A and B demonstrate 1D measurements showing the largest overall tumor diameter (cm) and largest enhancing tumor diameter (cm) represented by the red line. Figures C and D show the 2D tumor measurement methods and represent the maximum cross-sectional area (cm2) and maximum enhancing tumor area (cm2). E Segmentation of the tumor (3D reconstruction in red) showing the total tumor volume (cm3) in relation to

the total liver volume (cm3), shown by the yellow outline. F Assessing enhancing tumor volume (cm3). Dark-blue regions of the color map represent necrotic tissue, red regions show viable tumor tissue, as described in previous literature 19. The region of interest (ROI) that is represented by the green 1 cm3 box is used as the relative baseline enhancement of healthy liver parenchyma in order to calculate the differential enhancement within the segmentation-mask of the tumor.

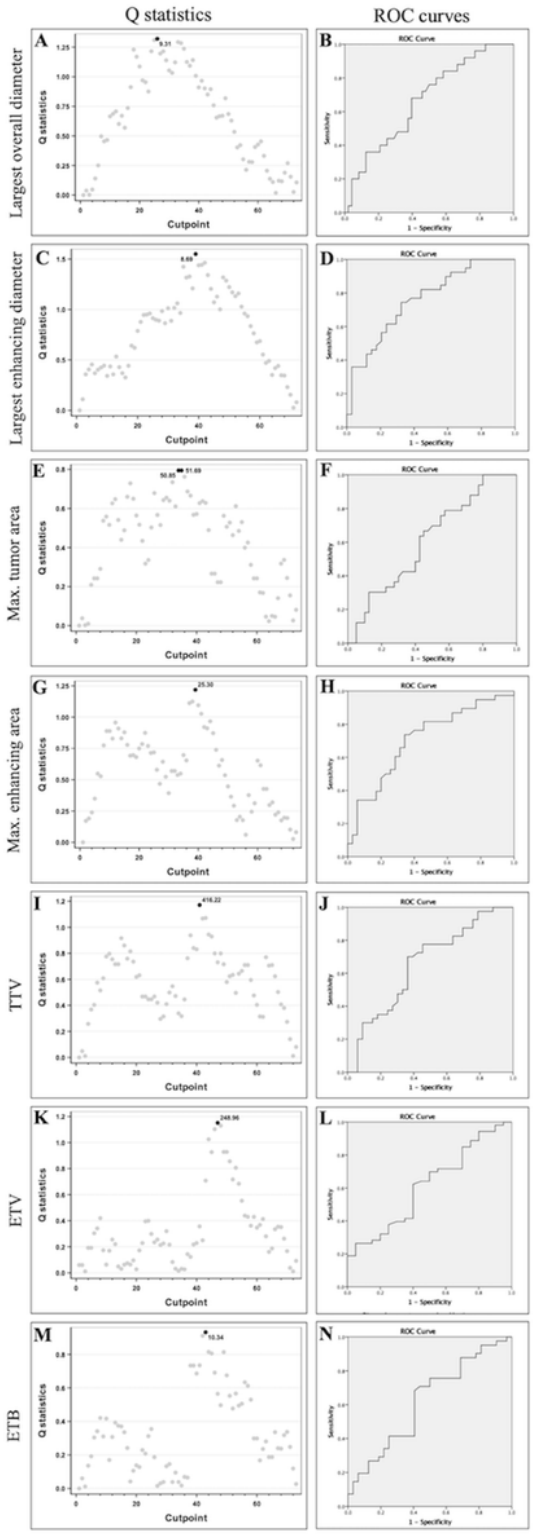

Figure 3

A & B. Based on Q statistics and ROC curve analysis, the cutoff point for the largest overall tumor diameter was determined as 9.3 cm with an AUC of 0.664. C & D. Q statistics and ROC curve analysis resulted in a cutoff value of 8.5 cm for the largest enhancing tumor diameter (AUC=0.759). E & F. Based on Q statistics and ROC curve analysis, the cutoff value for the maximum cross-sectional tumor area was determined as 50.0 cm2, with an AUC of 0.611. G &H. Q statistics and ROC curve analysis determined a cutoff value of 25.0 cm2 for the maximum enhancing tumor area (AUC=0.708). I &J. ROC curve analysis demonstrated a cutoff value of 410.0 cm3 for the total tumor volume with an AUC of 0.655. K&L. Based on Q statistics and ROC curve analysis, the cutoff point for the enhancing tumor volume was determined as 275.0 cm3 (AUC=0.612). M &N. Q statistics and ROC curve analysis determined a cutoff value of 10.0% for the enhancing tumor burden (AUC=0.620).

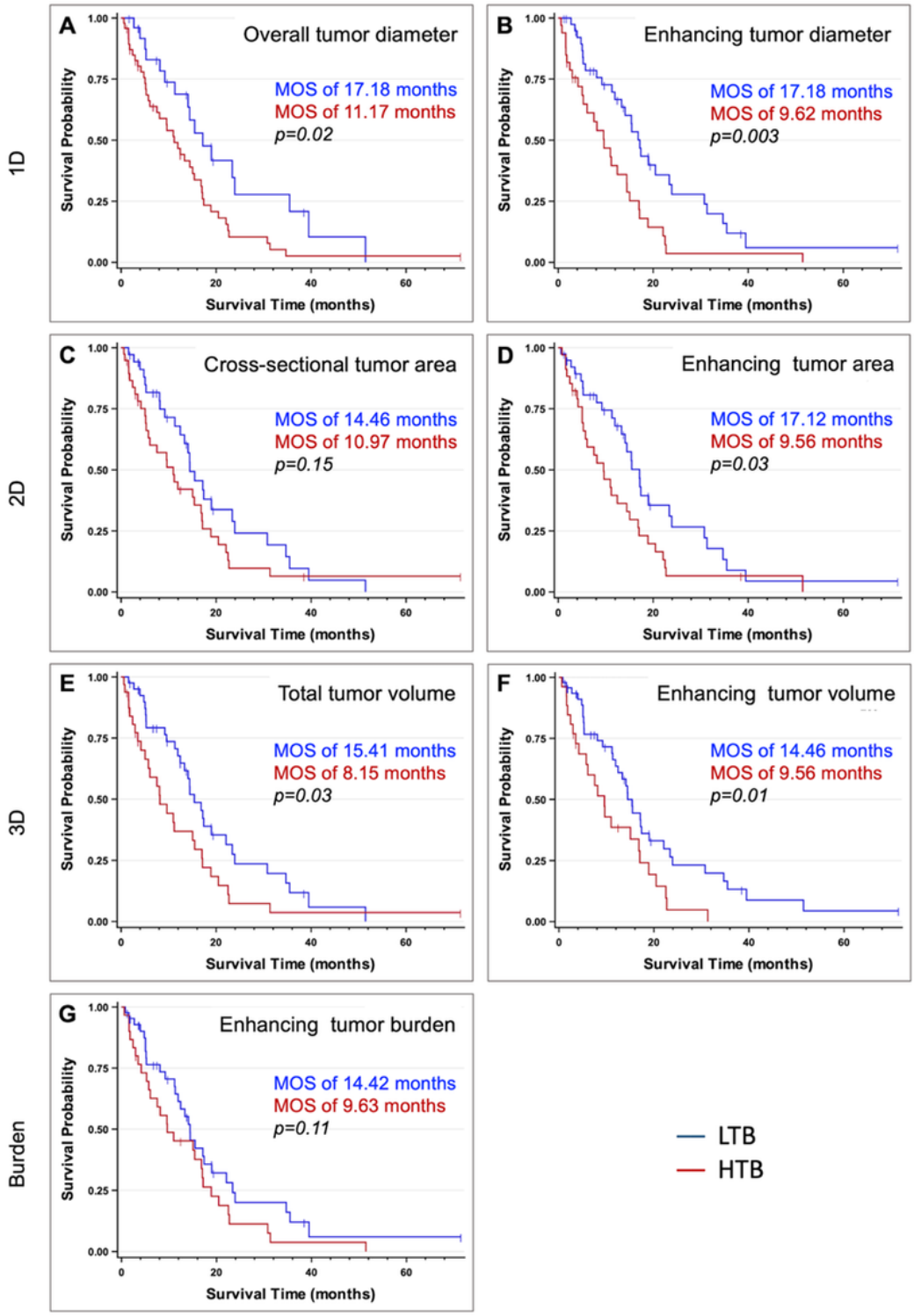

Figure 4

Kaplan-Meier analysis for overall survival calculated for each tumor burden assessment method after categorizing the ICC patients into two groups of low tumor burden (LTB) and high tumor burden (HTB). A and B show 1D based tumor assessment methods; the largest overall tumor diameter and largest enhancing tumor diameter. A. ICC patients with largest overall tumor diameter of ≤ 9.3 cm were categorized into the LTB group. There was significant difference between survival curves of the LTB and

HTB groups based on Log-rank test (p = 0.02). B. Patients with the largest enhancing tumor diameter of ≤ 8.5 cm were enrolled into the LTB group. A significant separation of survival curves between the LTB and HTB groups is shown with p = 0.003. C and D compare survival curves of the LTB and HTB groups when using the 2D tumor assessment methods, maximum cross-sectional tumor area and maximum enhancing tumor area. C. The LTB group includes patients with a tumor burden of ≤50.0 cm2 for maximum cross-sectional area. Log-rank test showed no significant separation between survival curves of the LTB and HTB groups (p = 0.15). D. For maximum enhancing tumor area, categorization into the LTB group was conducted when the maximum enhancing tumor area was ≤ 25.0 cm2. Log-rank test demonstrates a p = 0.03 between survival curves for the LTB and HTB groups. E, F, and G present Kapan-Meier curves when using 3D quantitative tumor analysis. E. Categorizing LTB according to assessment of total tumor volume was done when tumor burden was ≤ 410 cm3. Log-rank test showed a p = 0.03 between Kaplan-Meier curves of LTB and HTB. F. The LTB group was composed of ICC patients with enhancing tumor volume of ≤ 275 cm3 (p = 0.01 between survival curves of the LTB and HTB groups). G. When using enhancing tumor burden, patients were stratified to LTB when enhancing tumor burden was ≤ 10.0%. A p = 0.11 was achieved in log-rank test between survival curves of the LTB and HTB groups. MOS: Median overall survival.